

DEEP REINFORCEMENT LEARNING IN PARAMETERIZED ACTION SPACE

Matthew Hausknecht

Department of Computer Science
University of Texas at Austin
mhauskn@cs.utexas.edu

Peter Stone

Department of Computer Science
University of Texas at Austin
pstone@cs.utexas.edu

ABSTRACT

Recent work has shown that deep neural networks are capable of approximating both value functions and policies in reinforcement learning domains featuring continuous state and action spaces. However, to the best of our knowledge no previous work has succeeded at using deep neural networks in structured (parameterized) continuous action spaces. To fill this gap, this paper focuses on learning within the domain of simulated RoboCup soccer, which features a small set of discrete action types, each of which is parameterized with continuous variables. The best learned agents can score goals more reliably than the 2012 RoboCup champion agent. As such, this paper represents a successful extension of deep reinforcement learning to the class of parameterized action space MDPs.

1 INTRODUCTION

This paper extends the Deep Deterministic Policy Gradients (DDPG) algorithm (Lillicrap et al., 2015) into a parameterized action space. We document a modification to the published version of the DDPG algorithm: namely bounding action space gradients. We found this modification necessary for stable learning in this domain and will likely be valuable for future practitioners attempting to learn in continuous, bounded action spaces.

We demonstrate reliable learning, from scratch, of RoboCup soccer policies capable of goal scoring. These policies operate on a low-level continuous state space and a parameterized-continuous action space. Using a single reward function, the agents learn to locate and approach the ball, dribble to the goal, and score on an empty goal. The best learned agent proves more reliable at scoring goals, though slower, than the hand-coded 2012 RoboCup champion.

RoboCup 2D Half-Field-Offense (HFO) is a research platform for exploring single agent learning, multi-agent learning, and adhoc teamwork. HFO features a low-level continuous state space and parameterized-continuous action space. Specifically, the parameterized action space requires the agent to first select the type of action it wishes to perform from a discrete list of high level actions and then specify the continuous parameters to accompany that action. This parameterization introduces structure not found in a purely continuous action space.

The rest of this paper is organized as follows: the HFO domain is presented in Section 2. Section 3 presents background on deep continuous reinforcement learning including detailed actor and critic updates. Section 5 presents a method of bounding action space gradients. Section 6 covers experiments and results. Finally, related work is presented in Section 8 followed by conclusions.

2 HALF FIELD OFFENSE DOMAIN

RoboCup is an international robot soccer competition that promotes research in AI and robotics. Within RoboCup, the *2D simulation league* works with an abstraction of soccer wherein the players, the ball, and the field are all 2-dimensional objects. However, for the researcher looking to quickly prototype and evaluate different algorithms, the full soccer task presents a cumbersome prospect: full games are lengthy, have high variance in their outcome, and demand specialized handling of rules such as free kicks and offsides.

The Half Field Offense domain abstracts away the difficulties of full RoboCup and exposes the experimenter only to core decision-making logic, and to focus on the most challenging part of a RoboCup 2D game: scoring and defending goals. In HFO, each agent receives its own state sensations and must independently select its own actions. HFO is naturally characterized as an episodic multi-agent POMDP because of the sequential partial observations and actions on the part of the agents and the well-defined episodes which culminate in either a goal being scored or the ball leaving the play area. To begin each episode, the agent and ball are positioned randomly on the offensive half of the field. The episode ends when a goal is scored, the ball leaves the field, or 500 timesteps pass. Example videos of Half Field Offense games may be viewed at: <https://vid.me/sNev> <https://vid.me/JQTW> <https://vid.me/1b5D>. The following subsections introduce the low-level state and action space used by agents in this domain.

2.1 STATE SPACE

The agent uses a low-level, egocentric viewpoint encoded using 58 continuously-valued features. These features are derived through Helios-Agent2D’s (Akiyama, 2010) world model and provide angles and distances to various on-field objects of importance such as the ball, the goal, and the other players. Figure 1 depicts the perceptions of the agent. The most relevant features include: Agent’s position, velocity, and orientation, and stamina; Indicator if the agent is able to kick; Angles and distances to the following objects: Ball, Goal, Field-Corners, Penalty-Box-Corners, Teammates, and Opponents. A full list of state features may be found at <https://github.com/mhauskn/HFO/blob/master/doc/manual.pdf>.

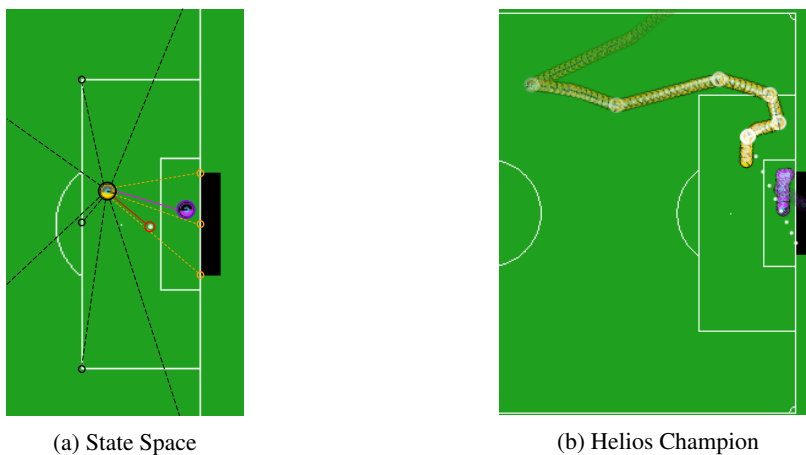


Figure 1: **Left:** HFO State Representation uses a low-level, egocentric viewpoint providing features such as distances and angles to objects of interest like the ball, goal posts, corners of the field, and opponents. **Right:** Helios handcoded policy scores on a goalie. This 2012 champion agent forms a natural (albeit difficult) baseline of comparison.

2.2 ACTION SPACE

Half Field Offense features a low-level, parameterized action space. There are four mutually-exclusive discrete actions: Dash, Turn, Tackle, and Kick. At each timestep the agent must select one of these four to execute. Each action has 1-2 continuously-valued parameters which must also be specified. An agent must select both the discrete action it wishes to execute as well as the continuously valued parameters required by that action. The full set of parameterized actions is:

Dash(power, direction): Moves in the indicated direction with a scalar power in $[0, 100]$. Movement is faster forward than sideways or backwards. **Turn(direction):** Turns in indicated direction. **Tackle(direction):** Contests the ball by moving in the indicated direction. This action is only useful when playing against an opponent. **Kick(power, direction):** Kicks the ball in the indicated direction with a scalar power in $[0, 100]$. All directions are parameterized in the range of $[-180, 180]$ degrees.

2.3 REWARD SIGNAL

True rewards in the HFO domain come from winning full games. However, such a reward signal is far too sparse for learning agents to gain traction. Instead we introduce a hand-crafted reward signal with four components: **Move To Ball Reward** provides a scalar reward proportional to the change in distance between the agent and the ball $d(a, b)$. An additional reward \mathbb{I}^{kick} of 1 is given the first time each episode the agent is close enough to kick the ball. **Kick To Goal Reward** is proportional to the change in distance between the ball and the center of the goal $d(b, g)$. An additional reward is given for scoring a goal \mathbb{I}^{goal} . A weighted sum of these components results in a single reward that first guides the agent close enough to kick the ball, then rewards for kicking towards goal, and finally for scoring. It was necessary to provide a higher gain for the kick-to-goal component of the reward because immediately following each kick, the move-to-ball component produces negative rewards as the ball moves away from the agent. The overall reward is as follows:

$$r_t = d_{t-1}(a, b) - d_t(a, b) + \mathbb{I}_t^{kick} + 3(d_{t-1}(b, g) - d_t(b, g)) + 5\mathbb{I}_t^{goal} \quad (1)$$

It is disappointing that reward engineering is necessary. However, the exploration task proves far too difficult to ever gain traction on a reward that consists only of scoring goals, because acting randomly is exceedingly unlikely to yield even a single goal in any reasonable amount of time. An interesting direction for future work is to find better ways of exploring large state spaces. One recent approach in this direction, Stadie et al. (2015) assigned exploration bonuses based on a model of system dynamics.

3 BACKGROUND: DEEP REINFORCEMENT LEARNING

Deep neural networks are adept general purpose function approximators that have been most widely used in supervised learning tasks. Recently, however they have been applied to reinforcement learning problems, giving rise to the field of deep reinforcement learning. This field seeks to combine the advances in deep neural networks with reinforcement learning algorithms to create agents capable of acting intelligently in complex environments. This section presents background in deep reinforcement learning in continuous action spaces. The notation closely follows that of Lillicrap et al. (2015).

Deep, model-free RL in discrete action spaces can be performed using the Deep Q-Learning method introduced by Mnih et al. (2015) which employs a single deep network to estimate the value function of each discrete action and, when acting, selects the maximally valued output for a given state input. Several variants of DQN have been explored. Narasimhan et al. (2015) used decaying traces, Hausknecht & Stone (2015) investigated LSTM recurrency, and van Hasselt et al. (2015) explored double Q-Learning. These networks work well in continuous state spaces but do not function in continuous action spaces because the output nodes of the network, while continuous, are trained to output Q-Value estimates rather than continuous actions.

An Actor/Critic architecture (Sutton & Barto, 1998) provides one solution to this problem by decoupling the value learning and the action selection. Represented using two deep neural networks, the actor network outputs continuous actions while the critic estimates the value function. The actor network μ , parameterized by θ^μ , takes as input a state s and outputs a continuous action a . The critic network Q , parameterized by θ^Q , takes as input a state s and action a and outputs a scalar Q-Value $Q(s, a)$. Figure 2 shows Critic and Actor networks.

Updates to the critic network are largely unchanged from the standard temporal difference update used originally in Q-Learning (Watkins & Dayan, 1992) and later by DQN:

$$Q(s, a) = Q(s, a) + \alpha(r + \gamma \max_{a'} Q(s', a') - Q(s, a)) \quad (2)$$

Adapting this equation to the neural network setting described above results in minimizing a loss function defined as follows:

$$L_Q(s, a|\theta^Q) = \left(Q(s, a|\theta^Q) - (r + \gamma \max_{a'} Q(s', a'|\theta^Q)) \right)^2 \quad (3)$$

However, in continuous action spaces, this equation is no longer tractable as it involves maximizing over next-state actions a' . Instead we ask the actor network to provide a next-state action $a' = \mu(s'|\theta^\mu)$. This yields a critic loss with the following form:

$$L_Q(s, a|\theta^Q) = \left(Q(s, a|\theta^Q) - (r + \gamma Q(s', \mu(s'|\theta^\mu)|\theta^Q)) \right)^2 \quad (4)$$

The value function of the critic can be learned by gradient descent on this loss function with respect to θ^Q . However, the accuracy of this value function is highly influenced by the quality of the actor's policy, since the actor determines the next-state action a' in the update target.

The critic's knowledge of action values is then harnessed to learn a better policy for the actor. Given a sample state, the goal of the actor is to minimize the difference between its current output a and the optimal action in that state a^* .

$$L_\mu(s|\theta^\mu) = (a - a^*)^2 = (\mu(s|\theta^Q) - a^*)^2 \quad (5)$$

The critic may be used to provide estimates of the quality of different actions but naively estimating a^* would involve maximizing the critic's output over all possible actions: $a^* \approx \arg \max_a Q(s, a|\theta^Q)$. Instead of seeking a global maximum, the critic network can provide gradients which indicate directions of change, in action space, that lead to higher estimated Q-Values: $\nabla_a Q(s, a|\theta^Q)$. To obtain these gradients requires a single backward pass over the critic network, much faster than solving an optimization problem in continuous action space. Note that these gradients are not the common gradients with respect to parameters. Instead these are gradients with respect to inputs, first used in this way by NFQCA (Hafner & Riedmiller, 2011). To update the actor network, these gradients are placed at the actor's output layer (in lieu of targets) and then back-propagated through the network. For a given state, the actor is run forward to produce an action that the critic evaluates, and the resulting gradients may be used to update the actor:

$$\nabla_{\theta^\mu} \mu(s) = \nabla_a Q(s, a|\theta^Q) \nabla_{\theta^\mu} \mu(s|\theta^\mu) \quad (6)$$

Alternatively one may think about these updates as simply interlinking the actor and critic networks: On the forward pass, the actor's output is passed forward into the critic and evaluated. Next, the estimated Q-Value is backpropagated through the critic, producing gradients $\nabla_a Q$ that indicate how the action should change in order to increase the Q-Value. On the backwards pass, these gradients flow from the critic through the actor. An update is then performed only over the actor's parameters. Figure 2 shows an example of this update.

3.1 STABLE UPDATES

Updates to the critic rely on the assumption that the actor's policy is a good proxy for the optimal policy. Updates to the actor rest on the assumption that the critic's gradients, or suggested directions for policy improvement, are valid when tested in the environment. It should come as no surprise that several techniques are necessary to make this learning process stable and convergent.

Because the critic's policy $Q(s, a|\theta^Q)$ influences both the actor and critic updates, errors in the critic's policy can create destructive feedback resulting in divergence of the actor, critic, or both. To resolve this problem Mnih et al. (2015) introduce a Target-Q-Network Q' , a replica of the critic network that changes on a slower time scale than the critic. This target network is used to generate next state targets for the critic update (Equation 4). Similarly a Target-Actor-Network μ' combats quick changes in the actor's policy.

The second stabilizing influence is a replay memory \mathcal{D} , a FIFO queue consisting of the agent's latest experiences (typically one million). Updating from mini-batches of experience sampled uniformly from this memory reduces bias compared to updating exclusively from the most recent experiences.

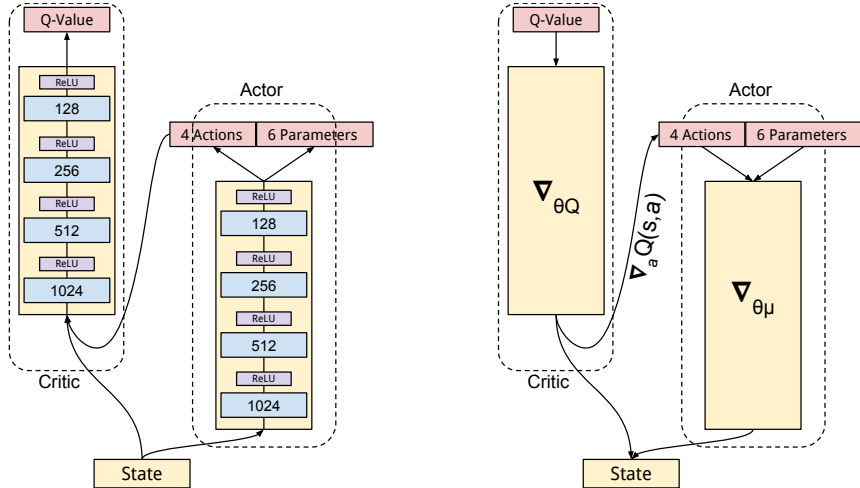


Figure 2: **Actor-Critic architecture (left)**: actor and critic networks may be interlinked, allowing activations to flow forwards from the actor to the critic and gradients to flow backwards from the critic to the actor. The gradients coming from the critic indicate directions of improvement in the continuous action space and are used to train the actor network without explicit targets. **Actor Update (right)**: Backwards pass generates critic gradients $\nabla_a Q(s, a|\theta^Q)$ w.r.t. the action. These gradients are back-propagated through the actor resulting in gradients w.r.t. parameters ∇_{θ^μ} which are used to update the actor. Critic gradients w.r.t. parameters ∇_{θ^Q} are ignored during the actor update.

Employing these two techniques the critic loss in Equation 4 and actor update in Equation 5 can be stably re-expressed as follows:

$$L_Q(\theta^Q) = \mathbb{E}_{(s_t, a_t, r_t, s_{t+1}) \sim \mathcal{D}} \left[\left(Q(s_t, a_t) - (r_t + \gamma Q'(s_{t+1}, \mu'(s_{t+1}))) \right)^2 \right] \quad (7)$$

$$\nabla_{\theta^\mu} \mu = \mathbb{E}_{s_t \sim \mathcal{D}} \left[\nabla_a Q(s_t, a|\theta^Q) \nabla_{\theta^\mu} \mu(s_t) \Big|_{a=\mu(s_t)} \right] \quad (8)$$

Finally, these updates are applied to the respective networks, where α is a per-parameter step size determined by the gradient descent algorithm. Additionally, the target-actor and target-critic networks are updated to smoothly track the actor and critic using a factor $\tau \ll 1$:

$$\begin{aligned} \theta^Q &= \theta^Q + \alpha \nabla_{\theta^Q} L_Q(\theta^Q) \\ \theta^\mu &= \theta^\mu + \alpha \nabla_{\theta^\mu} \mu \\ \theta^{Q'} &= \tau \theta^Q + (1 - \tau) \theta^{Q'} \\ \theta^{\mu'} &= \tau \theta^\mu + (1 - \tau) \theta^{\mu'} \end{aligned} \quad (9)$$

One final component is an adaptive learning rate method such as ADADELTA (Zeiler, 2012), RMSPROP (Tieleman & Hinton, 2012), or ADAM (Kingma & Ba, 2014).

3.2 NETWORK ARCHITECTURE

Shown in Figure 2, both the actor and critic employ the same architecture: The 58 state inputs are processed by four fully connected layers consisting of 1024-512-256-128 units respectively. Each fully connected layer is followed by a rectified linear (ReLU) activation function with negative slope 10^{-2} . Weights of the fully connected layers use Gaussian initialization with a standard deviation of 10^{-2} . Connected to the final inner product layer are two linear output layers: one for the four

discrete actions and another for the six parameters accompanying these actions. In addition to the 58 state features, the critic also takes as input the four discrete actions and six action parameters. It outputs a single scalar Q-value. We use the ADAM solver with both actor and critic learning rate set to 10^{-3} . Target networks track the actor and critic using a $\tau = 10^{-4}$. Complete source code for our agent is available at <https://github.com/mhauskn/dqn-hfo> and for the HFO domain at <https://github.com/mhauskn/HFO/>. Having introduced the background of deep reinforcement learning in continuous action space, we now present the parameterized action space.

4 PARAMETERIZED ACTION SPACE ARCHITECTURE

Following notation in (Masson & Konidaris, 2015), a Parameterized Action Space Markov Decision Process (PAMDP) is defined by a set of discrete actions $A_d = \{a_1, a_2, \dots, a_k\}$. Each discrete action $a \in A_d$ features m_a continuous parameters $\{p_1^a, \dots, p_{m_a}^a\} \in \mathbb{R}^{m_a}$. Actions are represented by tuples $(a, p_1^a, \dots, p_{m_a}^a)$. Thus the overall action space $A = \cup_{a \in A_d} (a, p_1^a, \dots, p_{m_a}^a)$.

In Half Field Offense, the complete parameterized action space (Section 2.2) is $A = (\text{Dash}, p_1^{\text{dash}}, p_2^{\text{dash}}) \cup (\text{Turn}, p_3^{\text{turn}}) \cup (\text{Tackle}, p_4^{\text{tackle}}) \cup (\text{Kick}, p_5^{\text{kick}}, p_6^{\text{kick}})$. The actor network in Figure 2 factors the action space into one output layer for discrete actions (Dash, Turn, Tackle, Kick) and another for all six continuous parameters $(p_1^{\text{dash}}, p_2^{\text{dash}}, p_3^{\text{turn}}, p_4^{\text{tackle}}, p_5^{\text{kick}}, p_6^{\text{kick}})$.

4.1 ACTION SELECTION AND EXPLORATION

Using the factored action space, deterministic action selection proceeds as follows: At each timestep, the actor network outputs values for each of the four discrete actions as well as six continuous parameters. The discrete action is chosen to be the maximally valued output $a = \max(\text{Dash}, \text{Turn}, \text{Tackle}, \text{Kick})$ and paired with associated parameters from the parameter output layer $(a, p_1^a, \dots, p_{m_a}^a)$. Thus the actor network simultaneously chooses which discrete action to execute and how to parameterize that action.

During training, the critic network receives, as input, the values of the output nodes of all four discrete actions and all six action parameters. We do not indicate to the critic which discrete action was actually applied in the HFO environment or which continuous parameters are associated with that discrete action. Similarly, when updating the actor, the critic provides gradients for all four discrete actions and all six continuous parameters. While it may seem that the critic is lacking crucial information about the structure of the action space, our experimental results in Section 6 demonstrate that the critic learns to provide gradients to the correct parameters of each discrete action.

Exploration in continuous action space differs from discrete space. We adapt ϵ -greedy exploration to parameterized action space: with probability ϵ , a random discrete action $a \in A_d$ is selected and the associated continuous parameters $\{p_1^a, \dots, p_{m_a}^a\}$ are sampled using a uniform random distribution. Experimentally, we anneal ϵ from 1.0 to 0.1 over the first 10,000 updates. Lillicrap et al. (2015) demonstrate that Ornstein-Uhlenbeck exploration is also successful in continuous action space.

5 BOUNDED PARAMETER SPACE LEARNING

The Half Field Offense domain bounds the range of each continuous parameter. Parameters indicating direction (e.g. Turn and Kick direction) are bounded in $[-180, 180]$ and parameters for power (e.g. Kick and Dash power) are bounded in $[0, 100]$. Without enforcing these bounds, after a few hundred updates, we observed continuous parameters routinely exceeding the bounds. If updates were permitted to continue, parameters would quickly trend towards astronomically large values. This problem stems from the critic providing gradients that encourage the actor network to continue increasing a parameter that already exceeds bounds. We explore three approaches for preserving parameters in their intended ranges:

Zeroing Gradients: Perhaps the simplest approach is to examine the critic’s gradients for each parameter and zero the gradients that suggest increasing/decreasing the value of a parameter that is already at the upper/lower limit of its range:

$$\nabla_p = \begin{cases} \nabla_p & \text{if } p_{\min} < p < p_{\max} \\ 0 & \text{otherwise} \end{cases} \quad (10)$$

Where ∇_p indicates the critic’s gradient with respect to parameter p , (e.g. $\nabla_p Q(s_t, a|\theta^Q)$) and p_{\min}, p_{\max}, p indicate respectively the minimum bound, maximum bound, and current activation of that parameter.

Squashing Gradients: A squashing function such as the hyperbolic tangent (\tanh) is used to bound the activation of each parameter. Subsequently, the parameters are re-scaled into their intended ranges. This approach has the advantage of not requiring manual gradient tinkering, but presents issues if the squashing function saturates.

Inverting Gradients: This approach captures the best aspects of the zeroing and squashing gradients, while minimizing the drawbacks. Gradients are downscaled as the parameter approaches the boundaries of its range and are inverted if the parameter exceeds the value range. This approach actively keeps parameters within bounds while avoiding problems of saturation. For example, if the critic continually recommends increasing a parameter, it will converge to the parameter’s upper bound. If the critic then decides to decrease that parameter, it will decrease immediately. In contrast, a squashing function would be saturated at the upper bound of the range and require many updates to decrease. Mathematically, the inverted gradient approach may be expressed as follows:

$$\nabla_p = \nabla_p \cdot \begin{cases} (p_{\max} - p)/(p_{\max} - p_{\min}) & \text{if } \nabla_p \text{ suggests increasing } p \\ (p - p_{\min})/(p_{\max} - p_{\min}) & \text{otherwise} \end{cases} \quad (11)$$

It should be noted that these approaches are not specific to HFO or parameterized action space. Any domain featuring a bounded-continuous action space will require a similar approach for enforcing bounds. All three approaches are empirically evaluated the next section.

6 RESULTS

We evaluate the zeroing, squashing, and inverting gradient approaches in the parameterized HFO domain on the task of approaching the ball and scoring a goal. For each approach, we independently train two agents. All agents are trained for 3 million iterations, approximately 20,000 episodes of play. Training each agent took three days on a NVidia Titan-X GPU.

Of the three approaches, only the inverting gradient shows robust learning. Indeed both inverting gradient agents learned to reliably approach the ball and score goals. None of the other four agents using the squashing or zeroing gradients were able to reliably approach the ball or score.

Further analysis of the squashing gradient approach reveals that parameters stayed within their bounds, but squashing functions quickly became saturated. The resulting agents take the same discrete action with the same maximum/minimum parameters each timestep. Given the observed proclivity of the critic’s gradients to push parameters towards ever larger/small values, it is no surprise that squashing function quickly become saturated and never recover.

Further analysis of the zeroing gradient approach reveals two problems: 1) parameters still overflow their bounds and 2) instability: While the gradient zeroing approach negates any direct attempts to increase a parameter p beyond its bounds, we hypothesize the first problem stems from gradients applied to other parameters $p_i \neq p$ which inadvertently allow parameter p to overflow. Empirically, we observed learned networks attempting to dash with a power of 120, more than the maximum of 100. It is reasonable for a critic network to encourage the actor to dash faster.

Unstable learning was observed in one of the two zeroing gradient agents. This instability is well captured in the Q-Values and critic losses shown in Figure 3. It’s not clear why this agent became unstable, but the remaining stable agent showed clear results of not learning.

These results highlight the necessity of non-saturating functions that effectively enforce action bounds. The approach of inverting gradients was observed to respect parameter boundaries (observed dash power reaches 98.8 out of 100) without saturating. As a result, the critic was able to effectively shape the actor’s policy. Further evaluation of the reliability and quality of the inverting-gradient policies is presented in the next section.

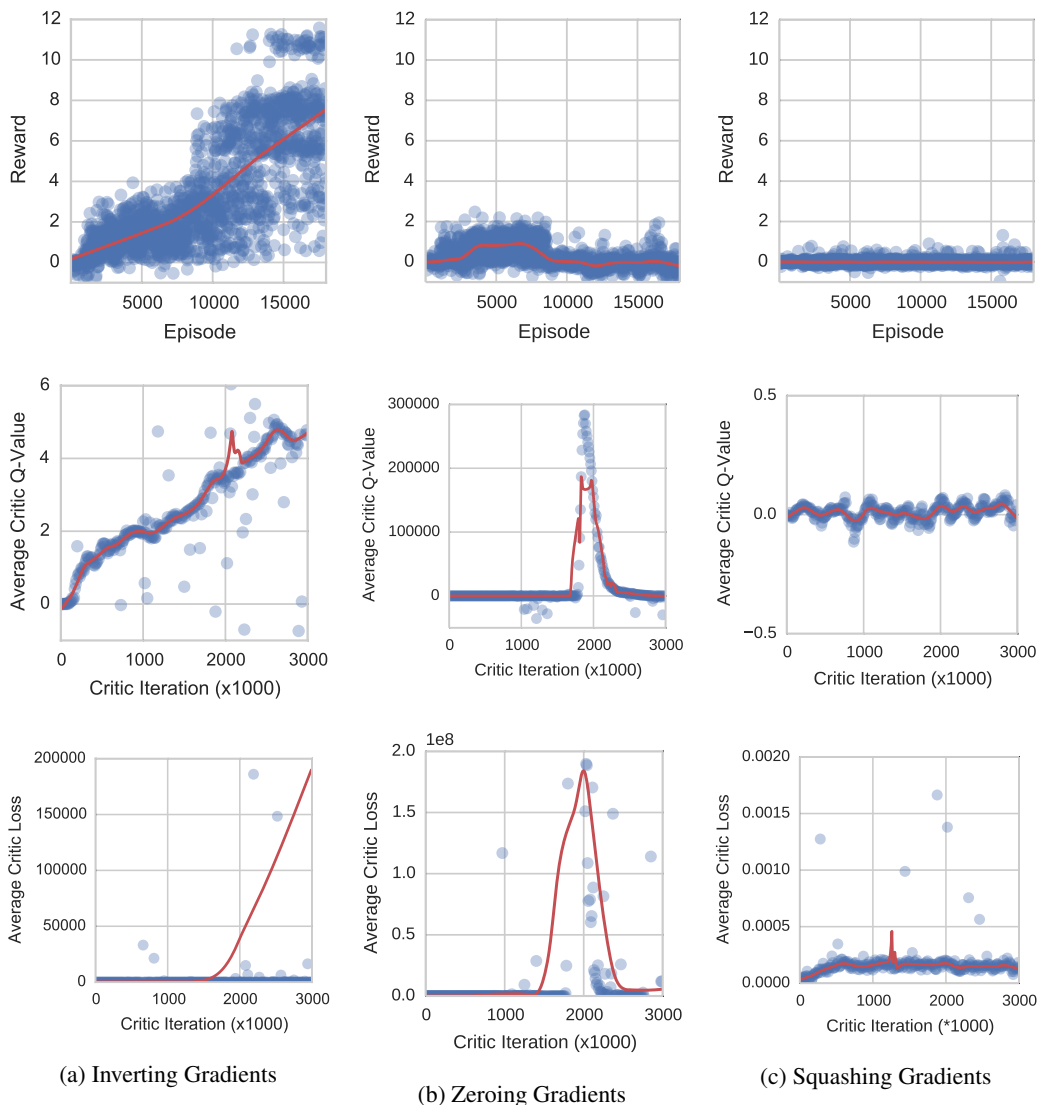


Figure 3: **Analysis of gradient bounding strategies:** The left/middle/right columns respectively correspond to the inverting/zeroing/squashing gradients approaches to handling bounded continuous actions. **First row** depicts learning curves showing overall task performance: Only the inverting gradient approach succeeds in learning the soccer task. **Second row** shows average Q-Values produced by the critic throughout the entire learning process: Inverting gradient approach shows smoothly increasing Q-Values. The zeroing approach shows astronomically high Q-Values indicating instability in the critic. The squashing approach shows stable Q-Values that accurately reflect the actor’s performance. **Third row** shows the average loss experienced during a critic update (Equation 7): As more reward is experienced critic loss is expected to rise as past actions are seen as increasingly sub-optimal. Inverting gradients shows growing critic loss with outliers accounting for the rapid increase nearing the right edge of the graph. Zeroing gradients approach shows unstably large loss. Squashing gradients never discovers much reward and loss stays near zero.

7 SOCCER EVALUATION

We further evaluate the inverting gradient agents by comparing them to an expert agent independently created by the Helios RoboCup-2D team. This agent won the 2012 RoboCup-2D world championship and source code was subsequently released (Akiyama, 2010). Thus, this hand-coded policy represents an extremely competent player and a high performance bar.

As an additional baseline we compare to a SARSA learning agent. State-Action-Reward-State-Action (SARSA) is an algorithm for model-free on-policy Reinforcement Learning Sutton & Barto (1998). The SARSA agent learns in a simplified version of HFO featuring high-level discrete actions for moving, dribbling, and shooting the ball. As input it is given continuous features that including the distance and angle to the goal center. Tile coding Sutton & Barto (1998) is used to discretize the state space. Experiences collected by playing the game are then used to bootstrap a value function.

To show that the deep reinforcement learning process is reliable, in addition to the previous two inverting-gradient agents we independently train another five inverting-gradient agents, for a total of seven agents DDPG₁₋₇. All seven agents learned to score goals. Comparing against the Helios’ champion agent, each of the learned agents is evaluated for 100 episodes on how quickly and reliably it can score.

Six of seven DDPG agents outperform the SARSA baseline, and remarkably, three of the seven DDPG agents score more reliably than Helios’ champion agent. Occasional failures of the Helios agent result from noise in the action space, which occasionally causes missed kicks. In contrast, DDPG agents learn to take extra time to score each goal, and become more accurate as a result. This extra time is reasonable considering DDPG is rewarded only for scoring and experiences no real pressure to score more quickly. We are encouraged to see that deep reinforcement learning can produce agents competitive with and even exceeding an expert hand-coded agent.

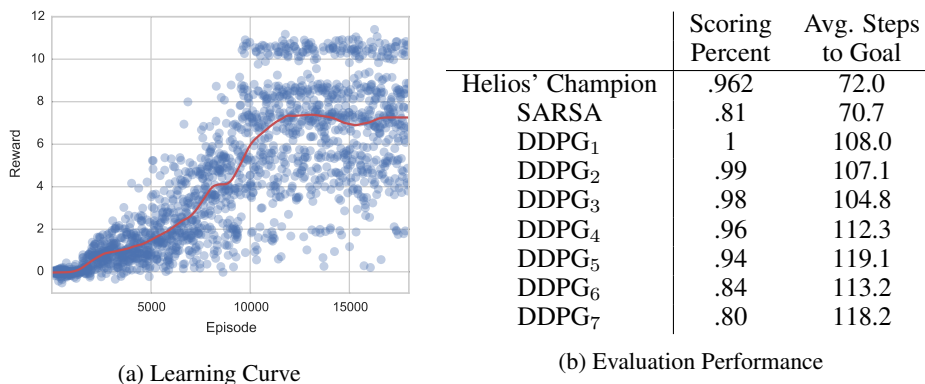


Figure 4: **Left:** Scatter plot of learning curves of DDPG-agents with Lowess curve. Three distinct phases of learning may be seen: the agents first get small rewards for approaching the ball (episode 1500), then learn to kick the ball towards the goal (episodes 2,000 - 8,000), and start scoring goals around episode 10,000. **Right:** DDPG-agents score nearly as reliably as expert baseline, but take longer to do so. A video of DDPG₁’s policy may be viewed at https://youtu.be/Ln0C1-jE_40.

8 RELATED WORK

RoboCup 2D soccer has a rich history of learning. In one of the earliest examples, Andre & Teller (1999) used Genetic Programming to evolve policies for RoboCup 2D Soccer. By using a sequence of reward functions, they first encourage the players to approach the ball, kick the ball, score a goal, and finally to win the game. Similarly, our work features players whose policies are entirely trained and have no hand-coded components. Our work differs by using a gradient-based learning method paired with using reinforcement learning rather than evolution.

Masson & Konidaris (2015) present a parameterized-action MDP formulation and approaches for model-free reinforcement learning in such environments. The core of this approach uses a parameterized policy for choosing which discrete action to select and another policy for selecting continuous parameters for that action. Given a fixed policy for parameter selection, they use Q-Learning to optimize the policy discrete action selection. Next, they fix the policy for discrete action selection and use a policy search method to optimize the parameter selection. Alternating these two learning phases yields convergence to either a local or global optimum depending on whether the policy search procedure can guarantee optimality. In contrast, our approach to learning in parameterized action space features a parameterized actor that learns both discrete actions and parameters and a parameterized critic that learns only the action-value function. Instead of relying on an external policy search procedure, we are able to directly query the critic for gradients. Finally, we parameterize our policies using deep neural networks rather than linear function approximation. Deep networks offer no theoretical convergence guarantees, but have a strong record of empirical success.

Experimentally, Masson & Konidaris (2015) examine a simplified abstraction of RoboCup 2D soccer which co-locates the agent and ball at the start of every trial and features a smaller action space consisting only of parameterized kick actions. However, they do examine the more difficult task of scoring on a keeper. Since their domain is hand-crafted and closed-source, it’s hard to estimate how difficult their task is compared to the goal scoring task in our paper.

Competitive RoboCup agents are primarily hand-coded but may feature components that are learned or optimized. MacAlpine et al. (2015) employed the layered-learning framework to incrementally learn a series of interdependent behaviors. Perhaps the best example of comprehensively integrating learning is the Brainstormers who, in competition, use a neural network to make a large portion of decisions spanning low level skills through high level strategy (Riedmiller et al., 2009; Riedmiller & Gabel, 2007). However their work was done prior to the advent of deep reinforcement learning, and thus required more constrained, focused training environments for each of their skills. In contrast, our study learns to approach the ball, kick towards the goal, and score, all within the context of a single, monolithic policy.

Deep learning methods have proven useful in various control domains. As previously mentioned DQN (Mnih et al., 2015) and DDPG (Lillicrap et al., 2015) provide great starting points for learning in discrete and continuous action spaces. Additionally, Levine et al. (2015) demonstrates the ability of deep learning paired with guided policy search to learn manipulation policies on a physical robot. The high requirement for data (in the form of experience) is a hurdle for applying deep reinforcement learning directly onto robotic platforms. Our work differs by examining an action space with latent structure and parameterized-continuous actions.

9 FUTURE WORK

The harder task of scoring on a goalie is left for future work. Additionally, the RoboCup domain presents many opportunities for multi-agent collaboration both in an adhoc-teamwork setting (in which a single learning agent must collaborate with unknown teammates) and true multi-agent settings (in which multiple learning agents must collaborate). Challenges in multi-agent learning in the RoboCup domain have been examined by prior work (Kalyanakrishnan et al., 2007) and solutions may translate into the deep reinforcement learning settings as well. Progress in this direction could eventually result in a team of deep reinforcement learning soccer players.

Another interesting possibility is utilizing the critic’s gradients with respect to state inputs $\nabla_s Q(s, a|\theta^Q)$. These gradients indicate directions of improvement in state space. An agent with a forward model may be able to exploit these gradients to transition into states which the critic finds more favorable. Recent developments in model-based deep reinforcement learning (Oh et al., 2015) show that detailed next state models are possible.

10 CONCLUSION

This paper has presented an agent trained exclusively with deep reinforcement learning which learns from scratch how to approach the ball, kick the ball to goal, and score. The best learned agent scores goals more reliably than a hand-coded expert policy. Our work does not address more challenging

tasks such as scoring on a goalie or cooperating with a team, but still represents a step towards fully learning complex RoboCup agents. More generally we have demonstrated the capability of deep reinforcement learning in parameterized action space.

To make this possible, we extended the DDPG algorithm (Lillicrap et al., 2015), by presenting an analyzing a novel approach for bounding the action space gradients suggested by the Critic. This extension is not specific to the HFO domain and will likely prove useful for any continuous, bounded action space.

ACKNOWLEDGMENTS

The authors wish to thank Yilun Chen. This work has taken place in the Learning Agents Research Group (LARG) at the Artificial Intelligence Laboratory, The University of Texas at Austin. LARG research is supported in part by grants from the National Science Foundation (CNS-1330072, CNS-1305287), ONR (21C184-01), AFRL (FA8750-14-1-0070), AFOSR (FA9550-14-1-0087), and Yujin Robot. Additional support from the Texas Advanced Computing Center, and Nvidia Corporation.

REFERENCES

- Akiyama, Hidehisa. Agent2d base code, 2010.
- Andre, David and Teller, Astro. Evolving Team Darwin United. *Lecture Notes in Computer Science*, 1604:346, 1999. ISSN 0302-9743. URL <http://link.springer-ny.com/link/service/series/0558/bibs/1604/16040346.htm>; <http://link.springer-ny.com/link/service/series/0558/papers/1604/16040346.pdf>.
- Hafner, Roland and Riedmiller, Martin. Reinforcement learning in feedback control. *Machine Learning*, 84(1-2):137–169, 2011. ISSN 0885-6125. doi: 10.1007/s10994-011-5235-x. URL <http://dx.doi.org/10.1007/s10994-011-5235-x>.
- Hausknecht, Matthew J. and Stone, Peter. Deep recurrent q-learning for partially observable mdps. *CoRR*, abs/1507.06527, 2015. URL <http://arxiv.org/abs/1507.06527>.
- Kalyanakrishnan, Shivaram, Liu, Yaxin, and Stone, Peter. Half field offense in RoboCup soccer: A multiagent reinforcement learning case study. In Lakemeyer, Gerhard, Sklar, Elizabeth, Sorenti, Domenico, and Takahashi, Tomoichi (eds.), *RoboCup-2006: Robot Soccer World Cup X*, volume 4434 of *Lecture Notes in Artificial Intelligence*, pp. 72–85. Springer Verlag, Berlin, 2007. ISBN 978-3-540-74023-0.
- Kingma, Diederik P. and Ba, Jimmy. Adam: A method for stochastic optimization. *CoRR*, abs/1412.6980, 2014. URL <http://arxiv.org/abs/1412.6980>.
- Levine, Sergey, Finn, Chelsea, Darrell, Trevor, and Abbeel, Pieter. End-to-end training of deep visuomotor policies. *CoRR*, abs/1504.00702, 2015. URL <http://arxiv.org/abs/1504.00702>.
- Lillicrap, T. P., Hunt, J. J., Pritzel, A., Heess, N., Erez, T., Tassa, Y., Silver, D., and Wierstra, D. Continuous control with deep reinforcement learning. *ArXiv e-prints*, September 2015.
- MacAlpine, Patrick, Depinet, Mike, and Stone, Peter. UT Austin Villa 2014: RoboCup 3D simulation league champion via overlapping layered learning. In *Proceedings of the Twenty-Ninth AAAI Conference on Artificial Intelligence (AAAI)*, January 2015.
- Masson, Warwick and Konidaris, George. Reinforcement learning with parameterized actions. *CoRR*, abs/1509.01644, 2015. URL <http://arxiv.org/abs/1509.01644>.
- Mnih, Volodymyr, Kavukcuoglu, Koray, Silver, David, Rusu, Andrei A., Veness, Joel, Bellemare, Marc G., Graves, Alex, Riedmiller, Martin, Fidjeland, Andreas K., Ostrovski, Georg, Petersen, Stig, Beattie, Charles, Sadik, Amir, Antonoglou, Ioannis, King, Helen, Kumaran, Dharshan, Wierstra, Daan, Legg, Shane, and Hassabis, Demis. Human-level control through deep reinforcement learning. *Nature*, 518(7540):529–533, February 2015. ISSN 0028-0836. doi: 10.1038/nature14236. URL <http://dx.doi.org/10.1038/nature14236>.

- Narasimhan, Karthik, Kulkarni, Tejas, and Barzilay, Regina. Language understanding for text-based games using deep reinforcement learning. *CoRR*, abs/1506.08941, 2015. URL <http://arxiv.org/abs/1506.08941>.
- Oh, Junhyuk, Guo, Xiaoxiao, Lee, Honglak, Lewis, Richard L., and Singh, Satinder P. Action-conditional video prediction using deep networks in atari games. *CoRR*, abs/1507.08750, 2015. URL <http://arxiv.org/abs/1507.08750>.
- Riedmiller, Martin, Gabel, Thomas, Hafner, Roland, and Lange, Sascha. Reinforcement learning for robot soccer. *Autonomous Robots*, 27(1):55–73, 2009. ISSN 0929-5593. doi: 10.1007/s10514-009-9120-4. URL <http://dx.doi.org/10.1007/s10514-009-9120-4>.
- Riedmiller, Martin A. and Gabel, Thomas. On experiences in a complex and competitive gaming domain: Reinforcement learning meets robocup. In *CIG*, pp. 17–23. IEEE, 2007. ISBN 1-4244-0709-5. URL <http://ieeexplore.ieee.org/xpl/mostRecentIssue.jsp?punumber=4219012>.
- Stadie, Bradley C., Levine, Sergey, and Abbeel, Pieter. Incentivizing exploration in reinforcement learning with deep predictive models. *CoRR*, abs/1507.00814, 2015. URL <http://arxiv.org/abs/1507.00814>.
- Sutton, Richard S. and Barto, Andrew G. *Reinforcement Learning: An Introduction*. MIT Press, 1998. ISBN 0262193981. URL <http://www.cs.ualberta.ca/%7Esutton/book/ebook/the-book.html>.
- Tieleman, T. and Hinton, G. Lecture 6.5—RmsProp: Divide the gradient by a running average of its recent magnitude. COURSERA: Neural Networks for Machine Learning, 2012.
- van Hasselt, Hado, Guez, Arthur, and Silver, David. Deep reinforcement learning with double q-learning. *CoRR*, abs/1509.06461, 2015. URL <http://arxiv.org/abs/1509.06461>.
- Watkins, Christopher J. C. H. and Dayan, Peter. Q-learning. *Machine Learning*, 8(3-4):279–292, 1992. doi: 10.1023/A:1022676722315. URL <http://jmvidal.cse.sc.edu/library/watkins92a.pdf>.
- Zeiler, Matthew D. ADADELTA: An adaptive learning rate method. *CoRR*, abs/1212.5701, 2012. URL <http://arxiv.org/abs/1212.5701>.